



**HAL**  
open science

# Adaptive Benefits of Storage Strategy and dual AMPK/TOR Signaling in Metabolic Stress Response

Benjamin Pfeuty, Quentin Thommen

► **To cite this version:**

Benjamin Pfeuty, Quentin Thommen. Adaptive Benefits of Storage Strategy and dual AMPK/TOR Signaling in Metabolic Stress Response. 2015. hal-01206918

**HAL Id: hal-01206918**

**<https://hal.science/hal-01206918>**

Preprint submitted on 29 Sep 2015

**HAL** is a multi-disciplinary open access archive for the deposit and dissemination of scientific research documents, whether they are published or not. The documents may come from teaching and research institutions in France or abroad, or from public or private research centers.

L'archive ouverte pluridisciplinaire **HAL**, est destinée au dépôt et à la diffusion de documents scientifiques de niveau recherche, publiés ou non, émanant des établissements d'enseignement et de recherche français ou étrangers, des laboratoires publics ou privés.

---

# Adaptive Benefits of Storage Strategy and dual AMPK/TOR Signaling in Metabolic Stress Response

Pfeuty Benjamin<sup>1,\*</sup> Thommen Quentin <sup>1</sup>

<sup>1</sup> Laboratoire de Physique des Lasers, Atomes et Molécules, Université de Lille Sciences et Technologies, CNRS ,Villeneuve d'Ascq, France

\* Benjamin.Pfeuty@univ-lille1.fr

## Abstract

Cellular metabolism must ensure that supply of nutrient meets the biosynthetic and bioenergetic needs. Cells have therefore developed sophisticated signaling and regulatory pathways in order to cope with dynamic fluctuations of both resource and demand and to regulate accordingly diverse anabolic and catabolic processes. Intriguingly, these pathways are organized around a relatively small number of regulatory hubs, such as the highly-conserved AMPK and TOR kinase families in eukaryotic cells. Here, the global metabolic adaptations upon dynamic environment are investigated using a prototypical model of regulated metabolism. In this model, the optimal enzyme profile as well as the underlying regulatory architecture are identified by combining perturbation and evolutionary methods. The results reveal the existence of distinct classes of adaptive strategies, which differ in the management of storage reserve depending on the intensity of the stress and in the regulation of ATP-producing reaction depending on the nature of the stress. The regulatory architecture that optimally implements these adaptive features is characterized by a crosstalk between two specialized signaling pathways, which bears close similarities with the sensing and regulatory properties of AMPK and TOR pathways.

## Introduction

To cope with environmental changes that impact their metabolism, living cells have evolved adaptive strategies consisting in sensing their extracellular or intracellular environment and regulating accordingly the activity of enzymes catalyzing metabolic reaction pathways. These strategic tasks involve only a few signaling pathways in spite of the huge number of enzyme-catalyzed metabolic pathways. In eukaryotes, the highly conserved AMPK (AMP-activated kinase) and TOR (target of rapamycin) families of protein kinase have crucial and numerous roles in nutrient and energy sensing, and in governing metabolic adaptations by regulating the expression and post-translational modifications of many metabolic enzymes [1–3]. Mammalian AMPK and its yeast and plant homologs Snf1 and SnRK1 are prone to be activated, allosterically or through phosphorylation, upon intracellular increases of AMP or ADP levels [4–6]. In turn, AMPK/Snf1/SnRK1 kinases tend to switch off anabolic pathways, including the biosynthesis of proteins, ribosomal RNA, carbohydrates or lipids while promoting their degradation through autophagy and fatty acid oxidation [7]. For its part, the TOR pathway is rather sensitive to intracellular levels of metabolites, especially amino acids, and

---

---

promotes growth by activating regulating biosynthetic pathways at the level of both transcriptional and translational machinery [8–10]. Besides their opposite roles in regulating biosynthetic pathways, both signaling pathways nevertheless share the same inclination to activate certain processes such as glycolysis or mitochondrial oxidative metabolism. For the latter, TOR promotes PGC-1 $\alpha$  [11], 4EBP dependent translational regulation [12] or TCA enzymes such as Glu dehydrogenase [13], and AMPK mediates as well the activation of mitochondrial enzymes mainly through pathways converging to PCG1 $\alpha$ /p [14, 15].

The crosstalk between AMPK and TOR signaling in sensing various intracellular cues and in regulating diverse anabolic and catabolic pathways raises a number of theoretical issues. The issue of intracellular sensing raises a difficult problem as these sensors are embedded into a global feedback architecture [16, 17]. As well, regulatory logic has been mainly studied for unbranched metabolic pathways [18–21] but much less for coupled metabolic pathways that both cooperate and compete for the utilization of internal resources. Besides the detailed schemes of sensing and regulatory mechanisms, several general questions arise about the adaptive logic of cell metabolism: How do signaling and regulatory strategies depend on the nature, frequency, duration, amplitude or randomness of environmental perturbations? What are the minimal requirements and the precise mechanisms that confer an adaptive benefit upon storage metabolism? The present study aims to address most of these issues through a minimal modeling approach.

Diverse computational modeling approaches have been developed to study the regulation of cell metabolism [22]. These approaches are generally based on a dual-level description made of a metabolic reaction network and an enzyme regulatory network. First, constraint-based stoichiometric models of genome-scale metabolic reaction network use steady-state assumptions and do not provide information on the enzymatic concentrations. Nevertheless, several extensions have attempted to overcome these limitations by incorporating a description of gene regulation [23], by considering enzyme costs and capacity constraints [24], by performing timescale separation hypothesis [24], or by using sensitivity analysis [25]. Second, metabolic control analysis is a powerful framework to study the response properties of complex metabolic systems to small changes of the kinetic parameters, which can be used to derive the optimal linear feedback regulation to static perturbation of steady state [26], and can be extended to the cases of non-steady state trajectories [27] or of time-dependent changes of kinetic parameters [28]. Although these two main modeling frameworks are well-adapted to determine optimal flux balance in detailed metabolic reaction networks, they remain dependent on steady-state or quasi-steady-state assumptions or on small perturbation approximations. A third approach consists in using simplified models depicting generic motifs (unbranched or cyclic pathways) or a prototypical metabolism, which allows to study regulation in simple resource allocation problem such as the switch from one to another substrate [30, 37], the switch between respiratory and fermentation metabolism [31], or the evolution of regulatory complexity [29]. The total number of kinetic parameters in these models is usually low enough to allow (i) for extensive parameter space exploration or (ii) for parameter optimization through evolutionary computation techniques, without necessarily requiring additional assumptions of steady state or of small enough environmental fluctuations.

In this paper, minimal modeling and evolutionary computation are exploited to investigate the regulated coordination of catabolic and anabolic processes, and to decipher the logic underlying the universal sensing and regulatory features of TOR and AMPK signaling pathway. To this purpose, we introduce a coarse-grained model of cell metabolism that recapitulates the main catabolic and anabolic pathways. Steady-state and perturbation analysis are first performed to identify the regulatory logic in response

---

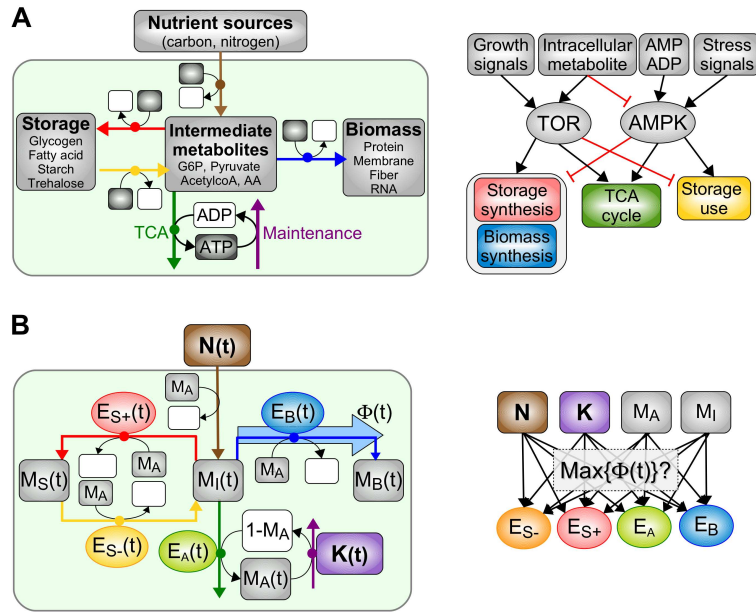


Figure 1: **Coarse-grained description of cell metabolism.** (A) Main anabolic and catabolic metabolic pathways regulated by TOR and AMPK/Snf1 signaling pathways. (B) Corresponding model including metabolic variable  $M_i$ , enzyme variable  $E_i$  and varying resource  $N$  and demand  $K$ , organized into a metabolic network (left) and a signaling/regulatory network (right).

to very slow or very small perturbations. Evolutionary computation is then applied to investigate adaptive strategy to a large range of perturbation amplitude and frequency, and to obtain the optimal enzyme time course and regulatory parameters. The results and the closing discussion emphasize the critical roles of storage metabolism, internal sensing and regulatory crosstalk, for metabolic adaptation to dynamic and complex environments.

## Methods

We consider a coarse-grained description of cell metabolism where nutrients are imported and catabolized into intermediate metabolites that can be either oxidized through the TCA cycle to produce ATP or utilized as precursors to build storage or biomass materials. In turn, ATP fuels most of the import, maintenance and biosynthetic processes (Fig. 1A). Each of these coarse-grained processes are based on a chain of reactions that is regulated by a pool of enzyme and is characterized with a global energy budget in terms of ATP cost or gain. Such schematic model of regulated metabolism can be translated into a biochemical reaction rate model (Fig. 1B and Table 1) where each macroprocess is modeled by a single reaction catalyzed by a single enzyme and consumes a given amount of ATP. The model therefore comprises different classes of variables and parameters : (i) metabolic variables  $M_j$  where  $j = I$  for intermediate,  $j = S$  for storage,  $j = B$  for biomass and  $j = A$  for ATP; (ii) regulatory variables  $E_j$  for the concentrations of enzymes catalyzing the  $j$ th reaction ( $j = A, B, S_+, S_-, T, M$ ); (iii) contextual/environmental variables,  $N$  for extracellular nutrient concentration and  $K$  for the energy demand; (iv) budget parameters  $k_j$  for the cost or gain in ATP of the  $j$ th reaction.

The time evolution of metabolic variables follows the differential equation system:

$$\frac{d\vec{M}}{dt} = \vec{F}(\vec{M}(t), \vec{E}(t), N(t), K(t)) \quad (1)$$

where  $\vec{F}$  is given in Table 1. It is to mention that two reactions are assumed to be catalyzed by constant enzyme level: (i) the nutrient transport reaction rate that is described by a non-regulated anisotropic diffusion process and (ii) the maintenance (i.e., housekeeping) reaction that is described as a zeroth order reaction and depends on the concentration of storage and enzyme (Table 1).

Table 1: **Biochemical reactions and parameter values.**

Nutrient transport	$N + k_T M_A + E_T \xleftrightarrow{*} M_I + k_T(1 - M_A) + E_T$ $v_1 = E_T M_A \mathcal{H}(N - M_I)$
ATP production	$M_I + k_A(1 - M_A) + E_A \rightarrow k_A M_A + E_A$ $v_2 = E_A(1 - M_A) M_I$
Biomass production	$M_I + k_B M_A + E_B \rightarrow M_B + k_B(1 - M_A) + E_B$ $v_3 = E_B M_A M_I$
Storage production	$M_I + k_{S+} M_A + E_{S+} \rightarrow M_S + k_{S+}(1 - M_A) + E_{S+}$ $v_4 = E_{S+} M_A M_I$
Storage degradation	$M_S + k_{S-} M_A + E_{S-} \rightarrow M_I + k_{S-}(1 - M_A) + E_{S-}$ $v_5 = E_{S-} M_A M_S$
Maintenance reaction	$M_A \rightarrow (1 - M_A)$ $v_6 = K_0 + K_S M_S + K_E \sum_i E_i$
Parameters	$k_A = 30; k_B = 5; k_T = 1; k_{S+} = 4; k_{S-} = 1$ $K_0 = 1; K_S = 0.01; K_E = 1; E_T = 0.5$
Rate equations	$\dot{M}_A = -k_T v_1 + k_A v_2 - k_B v_3 - k_{S+} v_4 - k_{S-} v_5 - v_6$ $\dot{M}_I = v_1 - v_2 - v_3 + v_5 - v_4; \dot{M}_S = v_4 - v_5; \dot{M}_B = v_3$

Reaction rates are based on first-order rate law, except the 0th order maintenance reaction rate. \* indicates that the reversible reaction occurs only for  $N > M_I$  with an Heavyside function  $\mathcal{H}$  in the rate law.  $1 - M_A$  denotes the converted form of  $M_A$  with a unit total pool concentration.

The sources of nonstationarity in the model are of two sorts : the changes in extra-cellular nutrient levels  $N(t)$  and the changes in energy demand  $K(t)$  as ATP-consuming cellular functions (stress management, motility, morphological changes...) are prone to be sensitive to environmental changes and transient in time. For simplicity, we consider sinusoidal variations of  $N(t)$  and  $K(t)$ :

$$N(t) = N_0 - \frac{(a_N \cos(\omega_N t)) - 1}{2} \quad (2)$$

$$K(t) = K_0 + \frac{(a_K \cos(\omega_K t)) - 1}{2} \quad (3)$$

where  $a_{N,K}$  are the perturbation amplitudes from such basal levels  $N_0$  and  $K_0$  and  $\omega_{N,K}$  are the perturbation frequencies. Given these nonstationary conditions, the optimization criterion for metabolic fitness is the time-averaged biomass production rate in the permanent regime:

$$\Phi = \frac{1}{T} \int_{t_0}^{t_0+T} E_B(t) M_I(t) M_A(t) dt \quad (4)$$

$$M_i(t_0 + T) = M_i(t_0), \quad \{i = I, A\}$$

where  $[t_0, t_0 + T]$  is the sampling time window and  $T = 2\pi/\omega$ .

---

## Metabolic parameter values

The prototypical model of metabolism depicted in Fig. 1 is not specific to a particular organism and does not take into account the diversity of nutrient sources, storage compounds and functional biomass compounds (e.g., DNA, RNA, proteins...). As a result, model parameters values are not necessarily related with known reaction rates and stoichiometries associated with a selected metabolic pathway. Nevertheless, the choice of parameter values has been made to match the order of magnitudes of some global or averaged biological quantities (Table 1). Parameter values are dependent on the concentration and time unit chosen. The assumption that the total concentration of the pool of adenylyl phosphate is constant and equal to 1 defines the unit of concentration. Because the experimentally measured value is of the order of 10mM (1mmol/L) and the molecular weight of ATP is 507g.mol<sup>-1</sup>, the concentration unit is set to 0.5g/L. The unit of time is given by the arbitrary choice that the basal decay rate of ATP is unit-normalized with  $K_0 = 1$ . The biological value of the basal consumption rate of ATP can be approximately derived from the respiratory rates  $J_{ATP} \sim 50\text{mM}\cdot\text{min}^{-1}$  measured in yeast cells in the stationary phase [33]. Given the concentration unit defined above and an ATP:ADP ratio of about  $\sim 5 : 1$ , the consumption rate would be  $6\text{min}^{-1}$  which corresponds to a time unit of 10s. This upper bound of ATP lifetime is consistent with the measured values of ATP turnover time of the magnitude of second in diverse growth conditions and species [32].

Parameters for ATP production and consumption are chosen from the global gain or cost of ATP associated with a whole metabolic process. The value for ATP gain associated with TCA cycle is set to  $k_A = 30$ , which is similar to the order of magnitude of 25g of ATP produced through the oxidation of 1g of acetyl COA (both metabolites have a similar molar mass). The value for ATP consumption associated with biomass production is set to  $k_B = 5$  as the minimal energy cost for protein synthesis is the 5 ATP hydrolyzed for each peptide bond formed, assuming that the molar mass of peptide is similar to that of ATP and neglecting other biosynthetic costs. The ATP cost for the whole process of storage production, maintenance and consumption depends on the type of storage compounds. We use the following arbitrary values  $k_{S_+} = 4$ ,  $k_{S_-} = 1$ ,  $K_S = 0.01$  and have checked a posteriori that storage content is lower than 10 times the adenylyl phosphate content  $M_s < 10$ , as starch or glycogen contents is usually limited to a maximum of a few percent of cell mass whereas ATP content of the magnitude of 0.1%. The parameter value  $E_T$  for nutrient import is based on the glucose import rate measured in budding yeast. Depending on the extracellular glucose concentration and the type of hexose transporter involved, glucose import rate can be estimated between 10 and  $100\text{min}^{-1}$  [34], which translates into  $0.5 < E_T < 5$  for the concentration and time units defined above.

## Regulatory parameter optimization

The search for regulatory parameters that shapes  $\vec{E}(t)$  so as to maximizes the flux  $\Phi$  in dynamic environments requires to use parameter optimization techniques. Perturbation methods are well adapted in the case of small enough environmental fluctuations. Environmental, enzyme and metabolic variables can be expanded up to first order  $x = x_0 + \epsilon x_1$  ( $x = M_i, E_i, N, K$ ) where first-order terms are real trigonometric polynomial functions:

$$x_1 = c_i + \sum_{i=1}^n a_i \cos(i\theta) + b_i \sin(i\theta) \quad (5)$$

where  $n = 1$  for  $x = E_i, N, K$  and otherwise undefined. By substituting Eq.5 into Eq.1 and Eq.4, the vector field  $\vec{F}$  and the objective function  $\Phi$  are expanded in power series

---

---

of  $\varepsilon$ , leading to a hierarchy of equations for  $\vec{M}$  and  $\Phi$  that can be solved recursively by using a formal calculus software. To the 0th order in  $\varepsilon$ , the steady state condition  $\vec{F}_0(\vec{M}_0, \vec{E}_0, \{N, K\}_0) = \vec{0}$  allows  $\vec{M}_0$  to be expressed as a function of  $\vec{E}_0$  and to be substituted into  $\Phi_0$ . Optimal enzyme parameters  $\vec{E}_0$  are obtained by finding the single local maximum of  $\Phi_0$  that satisfies  $\nabla \Phi_0(\vec{E}_0) = 0$  and  $\nabla^2 \Phi_0(\vec{E}_0) > 0$ . As well, solution of the linear equations at the following  $l$ th orders  $\vec{M}_l = \vec{F}_l$  allows to find asymptotic time-dependent solutions  $\vec{M}_l(t)$  as a function of trigonometric polynomial coefficients  $a$ ,  $b$  and  $c$  of  $\vec{E}_l$ , while the optimized coefficient are obtained again by maximizing  $\Phi_l$ .

In the case of large fluctuations  $N(t)$  and  $K(t)$ , perturbation method is substituted by evolution strategy optimization technique that is a class of evolutionary algorithm [35]. The optimization criterion is the maximization of the metabolic flux  $\Phi$  given by Eq.4 whereas the termination criterion depends on both the number of generation and a measure of evolution convergence.

## Results

### Steady-state metabolic adaptations: ATP homeostasis and metabolic collapse

In stationary condition defined by constant levels of nutrient  $N_0$ , energy demand  $K_0$  and enzymes  $\vec{E}_0$ , a stable metabolic state corresponds to a fixed point of Eq.1 with non-negative value of nutrients, metabolites, storage, ATP and ADP. However, for some range of values of  $N_0$ ,  $K_0$  and  $\vec{E}_0$ , a stable metabolic state may not exist, such that all phase space trajectories drift toward the region of negative ATP level ( $M_A < 0$ ), in which case metabolic death occurs. As mentioned in Methods section, an optimal stable metabolic steady state is defined for enzyme parameters  $\vec{E}_0$  that maximize the metabolic flux  $\Phi$  for any values  $N_0$  and  $K_0$  (Fig. 2). The optimal metabolic flux  $\Phi$  decreases with decreasing values of  $N_0$  and increasing values  $K_0$  to  $\Phi = 0$  at a threshold value  $N_{0,c}(K_0)$  and  $K_{0,c}(N_0)$  (Fig. 2A) beyond which metabolic death always occurs. This stress-induced decrease of  $\Phi$  is paralleled with a decay of biomass production enzyme  $E_{0,B}$  to 0 (Fig. 2B), while the ATP production enzyme  $E_{0,A}$  is either slightly increased or decreased depending on whether it is a nutrient stress or an energy stress, respectively (Fig. 2C). In this result, the smaller regulation of  $E_{0,A}$  compared to that of  $E_{0,B}$  reflects the imperative need to maintain relatively constant and high levels of ATP for survival at the expense of a much reduced biomass production and flux (Fig. 2D). Furthermore, the opposite regulation of  $E_{0,A}$  between the two types of stress reflects the fact that the many ATP-producing and ATP-consuming reactions can be differentially affected by the two stress types, such that stress-specific and finely-tuned regulation are required to reestablish ATP homeostasis. In contrast with these subtle mechanisms of ATP homeostasis, the optimal level of internal metabolites  $M_I$  roughly scales with external nutrients  $N_0$  (Fig. 2E). Finally, an expected feature of the optimal steady state is the absence of storage enzymes  $E_{0,S+/-} = 0$  as the processes of production, maintenance and degradation of storage generate metabolic costs in ATP and enzymes and any profits in stationary conditions. Note that even for the optimal enzyme parameters, a stable fixed point coexists with a saddle fixed point (Fig. 2F), such that transition to death can arise at the threshold condition  $K_{0,c}$  and  $N_{0,c}$  through a saddle-node bifurcation but also through transient perturbations, which is a critical feature for further investigations of the effect of dynamic fluctuations. Quantitatively, the value  $\Phi \sim 0.12$  obtained for  $N_0 = 1$  and the nutrient threshold of  $N_0 = 0.3$  corresponds to a doubling time of  $\sim 10$ h for an external glucose concentration of 25mM, which matches the order of magnitude

---

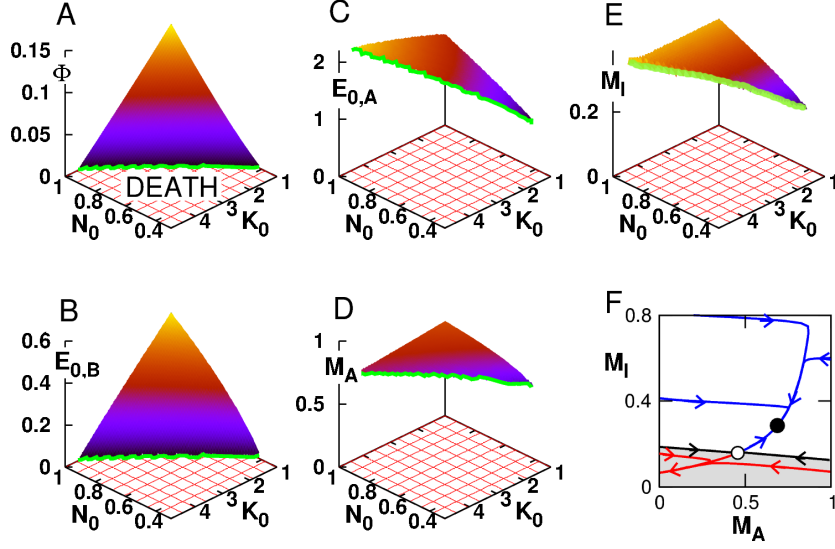


Figure 2: **Optimal steady-state solutions.** Properties of the optimal solution as a function of stationary parameters  $N_0$  and  $K_0$ : (A) Flux  $\Phi$  where green line corresponds to  $\Phi = 0$ ; (B-C) Stationary enzyme level  $E_{0,B}$  and  $E_{0,A}$ ; (D,E) Stable fixed point coordinate  $M_A$  and  $M_I$ ; (F) Example of phase space portrait and trajectories for  $N_0 = 0.8$  and  $K_0 = 2$  where black and white circles indicate stable and unstable fixed points and the black line separates the viability domain (white) and metabolic collapse domain (gray).

of experimental values [36].

## Dynamic metabolic adaptations: just-in-time and storage strategies

After having characterized the main features of the optimal metabolic steady state, the following step is to search for optimal enzyme profiles in response to nonstationary environmental conditions such as oscillations of  $N(t)$  and  $K(t)$  of amplitudes  $a_{N,K}$  given by Eq.2 (Fig. 3A). For simplicity, we assume a sinusoidal shape for  $\vec{E}(t)$

$$E_i(t) = e_{0,i}(1 + a_i \cos(\omega_{N,K}t + \varphi_i)) \quad (6)$$

The optimal values for  $e_{0,i}$ ,  $a_i$  and  $\varphi_i$  can first be derived for small amplitude oscillations  $a_i$  by using a perturbation method, and then obtained for any perturbation amplitude by using evolutionary methods (see Methods section). The results depicted in Fig. 3B shows that the optimal solutions are well predicted by the perturbation approach, up to relatively large stress amplitudes  $a_{N,K}$ , which can be explained by the almost linear relation between the metabolic flux and the parameter perturbation (Fig. 2A). For these optimal solutions, the enzyme oscillations display an increasing amplitude with perturbation amplitude and are in phase or antiphase with the perturbation depending on whether  $dE_{0,i}/dN$  and  $dE_{0,i}/dK$  are positive or negative in (Fig. 2B,C). The in-phase or anti-phase relationship between enzyme and perturbation oscillations is related with the assumption of a low perturbation frequency  $\omega_{N,K} = 0.01$  (i.e, dimensionalized period of  $T = 100\text{mn}$ ) that is much smaller than the natural frequency  $\omega_0$  of the metabolic system, while phase shifts would occur for  $\omega_{N,K} \sim \omega_0$ . This strategy bears



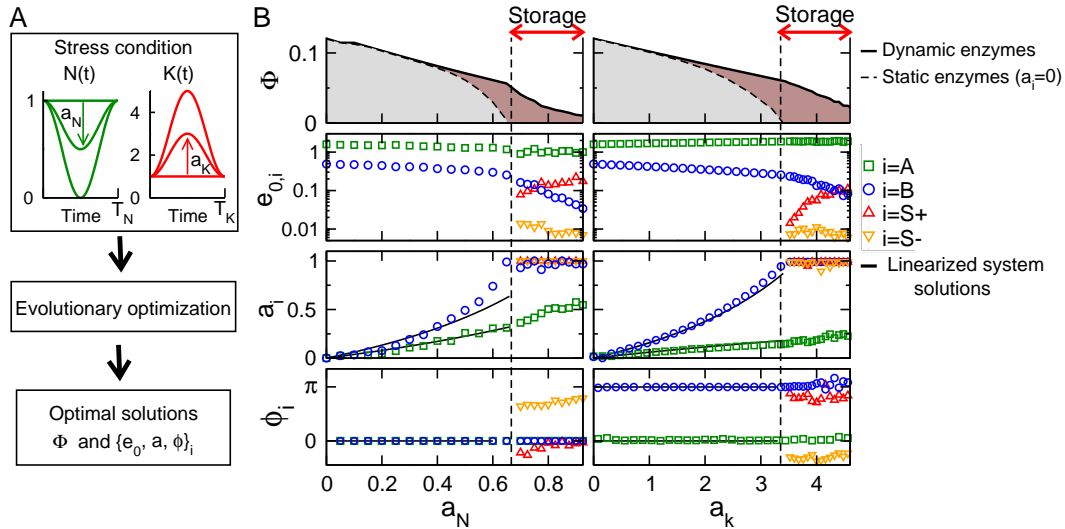


Figure 3: **Optimal enzyme profile in presence of time-dependent nutrient or energy stress.** (A) Simulation protocol to obtain optimal enzyme profile as a function of the stress condition. (B) Optimal solutions as a function of stress type and amplitude reveals the existence of storage-based solutions for large enough amplitude. Upper panel: Metabolic flux  $\Phi$ , mean enzyme level  $e_{0,i}$ , amplitude of enzyme oscillations  $a_i$ , phase of enzyme oscillations  $\varphi_i$ . Optimal enzyme profile obtained with evolution methods (colored point) are compared with small amplitude solutions obtained with perturbation methods (continuous lines).

similarities with so-called just-in-time or lean manufacturing strategy for production lines as enzymes must be produced and activated at the right time by maximizing the use of rate-limiting substrates while avoiding accumulating or stored parts. However, above some critical perturbation amplitude  $a_{i,c} > a_{i,c}$  ( $i = N, K$ ), the optimal solutions display qualitatively different properties characterized by a tight regulation of storage production and degradation ( $e_{0,S} > 0$ ,  $a_{S+}, a_{S-} = 1$  and  $\varphi_{S+} \sim \varphi_{S-} + \pi$ ).

These storage-based solutions occur for a given frequency range of oscillatory perturbations (Fig. 4A,B). The upper-bound frequency coincides with the undamped natural (also cutoff) frequency  $\omega_0$  of the low-pass second-order filter associated with the metabolic system  $\{M_A, M_I\}$  linearized around the steady state  $N_0 = k_0 = 1$ . The storage strategy thus confers a fitness benefit for slow variations of  $N(t)$  or  $K(t)$  below the thresholds  $N_{0,c}$  or  $K_{0,c}$ , which would not be filtered out and would induce metabolic death in the absence of slow storage cycles. In turn, the lower-bound frequency indicates that a too long stress requires to be anticipated with high storage reserves that comes with an unbearable cost and death. As a result, the precise values of this bound depends on the actual cost of storage production and maintenance.

The mechanism through which the accumulation and degradation of storage material buffer out slow environmental fluctuations can be captured by the low-pass filter component in presence of stationary levels of enzymes  $E_i(t) = E_{0,i}$  (Fig. 4C). The dominant cutoff frequency coincides with the environmental frequency for which the system has been optimized. The optimal profile of the enzymatic variables and the corresponding time course for metabolic variables depicted in Fig. 4D illustrate how the optimal solution coincides with a temporal management of storage material, in order to ensure that  $M_A$  and  $M_I$  remain in the viability domain (shown in Fig. 2F) so as to avoid metabolic collapse.

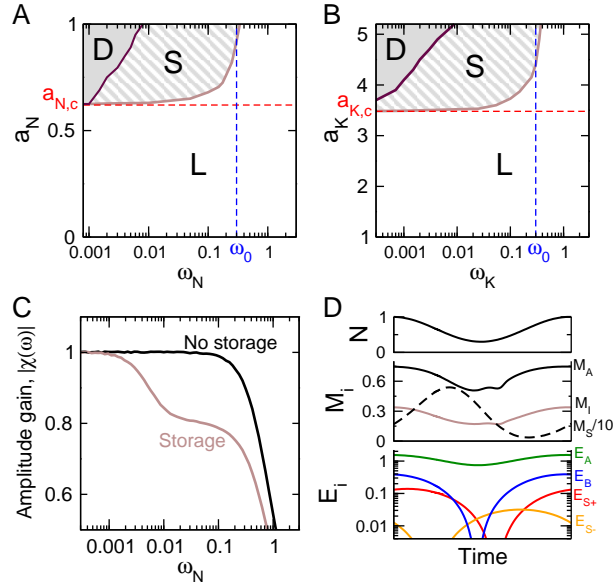


Figure 4: **Storage strategy.** (A,B) Distinct classes of optimal solutions (S: Storage; L: lean / no storage; D: Death) as a function of the type, the amplitude and the frequency of the stress condition. (C) Amplitude gain as a function of perturbation frequency in presence of static enzyme with and without storage reveals specific low-pass filtering properties. (D) Timecourse of metabolic and enzymatic variable illustrated for an optimal solution with nutrient stress  $\omega_N = 0.01$  and  $a_N = 0.75$ .

## Optimal signaling and regulation for dynamic adaptations to metabolic stress

The optimal oscillatory profiles of enzyme obtained for various nonstationary conditions provide guidance on the manner how these enzymes would be optimally regulated by specific signaling cues. For instance, the optimal phases of enzyme oscillations with respect to signal oscillations (see low panels of Fig. 3) are expected to predict whether these enzymes would be positively or negatively regulated by the signaling pathways sensitive to these signals. It remains however difficult to foresee which signaling cues and how many signaling pathways are required to regulate metabolism in an optimal manner. To address these issues, the metabolic network model given by Eq.1 is supplemented by a minimal description of the signaling pathways that regulate the time evolution of enzyme concentration :

$$\tau_i \frac{dE_i}{dt} = \mu_i \prod_{j=1}^{N_Y} f_{ij}(Y_j) - E_i \quad (7)$$

where  $Y_j$  is the signal input that can depend on any environmental or metabolic variables, and  $N_Y$  is the number of signaling pathway. The regulation function  $f_{ij}$  is described by a Hill function:

$$f_{ij}(x) = \frac{1 + \lambda_{ij} \left( \frac{x}{\theta_{ij}} \right)^{n_H}}{1 + \left( \frac{x}{\theta_{ij}} \right)^{n_H}} \quad (8)$$

where  $\mu_i$  is the basal activation rate of  $E_i$ ,  $\lambda_{ij}$  the  $Y_j$ -dependent activation ( $> 1$ ) or inactivation ( $< 1$ ) rate of  $E_i$  by  $Y_j$ ,  $\theta_{ij}$  the regulatory threshold (the inflection point of the response curve for  $n_H = 2$ ), and  $n_H$  is the Hill coefficient or slope factor that

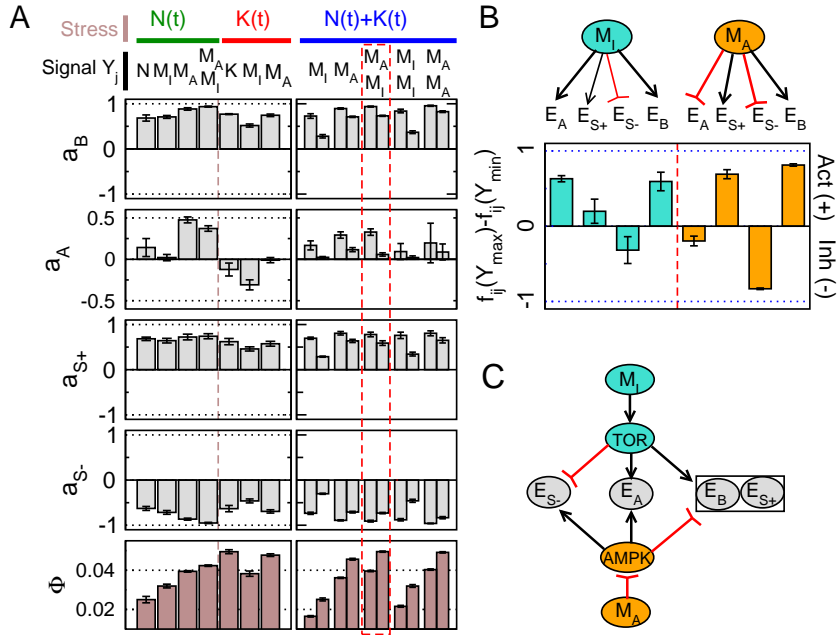


Figure 5: **Optimal signaling and regulatory pattern of enzyme in response to single or combined stress conditions.** (A) Enzyme amplitude (Eq. 9): average and variance values computed for the 20 better solutions over 40 evolutionary runs. Evolutionary optimization is made on the regulatory parameters  $\mu_i$ ,  $\lambda_{ij}$  and  $\theta_{ij}$  for two distinct and combined stress conditions ( $N(t)$ :  $N_0 = 1$ ,  $\omega_N = 0.01$ ,  $a_N = 0.7$ ,  $a_K = 0$ ;  $K(t)$ :  $N_0 = 1$ ,  $\omega_N = 0.01$ ,  $a_N = 0.$ ,  $a_K = 3.5$ ) and for various signals. For optimization in combined stress conditions (right panel), left versus right bars corresponds to enzyme amplitudes measured when exposed to a single stress,  $N(t)$  (left) or  $K(t)$  (right). (B) Optimal regulatory parameters  $f_{ij}(Y_{max}) - f_{ij}(Y_{min})$  represented as activatory or inhibitory regulations in presence of two signaling pathway and combined stress conditions (see dashed rectangle of (A)). (C) Corresponding regulatory scheme by assuming the existence of AMPK-like and TOR-like regulatory proteins.

is set to 2. Evolutionary optimization technique is applied to determine the regulatory parameters  $\mu_i$ ,  $\lambda_{ij}$  and  $\theta_{ij}$  that maximizes the flux. We use constant value  $\tau_i = 1$ , which would correspond to a rapid mode of regulation (e.g, post-translational), since, anyway, optimization leads to minimize  $\tau_i$  in the absence of synthesis and degradation costs for enzymes. To compare the optimal solutions obtained in the cases of oscillatory versus regulated enzymes, a generic quantity for enzyme amplitude is defined as,

$$a_i = \cos(\varphi) \frac{E_i^M - E_i^m}{E_i^M + E_i^m} \quad (9)$$

where  $\varphi = 2\pi(t'_{E_i} - t'_{K,N})/T$  corresponds to the phase of the enzyme response ( $t'_x$  is the time of the maximum of  $x(t)$ ). Optimization is first performed in presence of a single stress conditions ( $N(t)$  or  $K(t)$  with  $\omega_{N,K} = 0.01$ ) and a single signaling pathway  $N_Y = 1$  where  $Y_1$  is a function of  $N$ ,  $K$ ,  $M_I$  or  $M_A$  (Fig.5A, left panels). The sensing functions are  $Y(N) = N$ ,  $Y(M_I) = M_I$ ,  $Y(K) = 5 - K$  and  $Y(M_A) = 0.1 M_A / (1 - M_A)$  and have been chosen to display similar maximal and minimal values for  $Y$  given the stress intensities considered here.

Irrespective to the signaling cue, a stress associated with low levels of  $N$ ,  $M_I$  or  $M_A$  or high levels of  $K$  induces an inhibition of enzymes  $E_{S+}$ ,  $E_B$  and activation of  $E_{S-}$ ,

---

while it induces either an activation or an inactivation of  $E_A$  depending on whether it is an energy or a nutrient stress, respectively (Fig.5A, left panels). These tendencies are consistent with the optimal oscillatory pattern of enzyme (see Fig.3). However, both the strengths of regulation and the metabolic flux  $\Phi$  slightly depend on the type of signaling cues, which presumably reflects differences in the periodic time profile of  $Y_j(t)$  which can be more or less sinusoidal or distorted. The result that  $\Phi$  systematically augments by increasing the hill coefficient  $n_H$  (result not shown) or by increasing the number of signaling pathways  $N_Y$  is consistent with the notion that signaling complexity improves metabolic fitness through a refined control of enzyme time course in the absence of costs associated with increases of  $N_Y$  or  $n_H$ .

In the case where a single signaling pathway is optimized to maximize the sum of the flux for the two stress conditions (Fig.5A, right panels), the metabolic flux is decreased from 10% (for  $M_A$ ) to 40% (for  $M_I$ ) compared to the case where optimization is done for each stress condition separately. This result reflects the property that optimal regulation of  $E_A$  depends on the stress type, giving rise to a compromise solution of intermediate regulation of  $E_A$ . In contrast, optimization with two signaling pathways allows to recover the optimal fluxes obtained for each stress condition optimized separately with a single signaling pathway. This dual signaling and regulatory scheme shows a clear division of the sensing and regulatory task as the signaling sensitive to  $M_I$  inhibits  $E_A$  while the pathways sensitive to  $M_A$  activates  $E_A$  (Fig.5B), which is reminiscent to the acknowledged pattern of regulation by AMPK and TOR (Compare Fig.5C and Fig.1A). Besides their opposite regulation of  $E_A$ , the two signaling pathways also differ in the regulatory strength of storage enzyme, which also suggest a division of task based on the survival-growth dichotomy. The  $M_A$ -sensitive pathway is prone to lead to drastic metabolic adaptation upon severe stress, while the  $M_I$ -signaling pathway would rather achieve a more graded response to optimize the metabolic growth rate.

To summarize, the crosstalk between several signaling and regulatory pathways confers fitness advantages by refining the time profile of respective enzymes, but also by allowing a distribution of tasks when coping with different stress types and intensities.

## Discussion

The analysis of a coarse-grained model of cell metabolism reveals distinct adaptive strategies in changing environments, depending on the nature, the amplitude, and the timescale of environmental changes. In line with previous studies, adaptation to small environmental fluctuations only requires to be compensated in time by dynamically reallocating the enzyme resources [37, 38] by analogy with just-in-time manufacturing strategies [18]. In contrast, metabolic adaptation to large environmental fluctuations involves storage management's pathways in order to buffer out these fluctuations and protect cells against detrimental outcomes for survival. The buffer effect relies on a slow storage degradation process, providing a low-pass filtering's property to the metabolic system. In this process, a tight regulation of the storage's production and degradation is of critical importance to minimize the cost of production and of maintenance of storage material. A typical example of such adaptive mechanism is the regulation of starch, a major form of stored carbohydrate in plants: starch is accumulated during the day and remobilized at night at a rate which depends on the night length to support continued respiration [39]. In fact, different storage compounds may exhibit differential capacities in coping with rapid or slow changes of their environment, depending on the energetic and temporal constraints associated with their production, transport, reactivity, and degradation. Carbohydrates, for instance, are energy's stores less concentrated than triacylglycerols, but are more rapidly mobilized. The specific roles of glycogen and trehalose during the diauxic shift response and the quiescence starvation response in yeast

---

---

further suggest the existence of distinct and combined storage strategies depending on the mode of production and reactivity of storage compounds [40]. Finally, proteins and other macromolecular complexes also constitutes large reserves of recyclable material that can be catabolized through the process of autophagy [41]. This diversity of catabolic processes leave open the question of their coordination to resupply the biosynthetic precursors or the energetic compounds and to optimize survival at various timescales.

Optimal metabolic fitness in fluctuating environments requires a time-dependent regulation of storage material, but also of biosynthetic ATP-consuming processes and catabolic ATP-generating processes. While the biosynthetic machinery is switched off in any stress condition, the regulation of the ATP production through the TCA cycle is more subtle and is prone to depend on the nature of the stress. As a result, optimal regulation in various stress conditions tend to require a crosstalk between specialized signaling pathways that have both cooperative or opposing actions on selected enzymatic targets. The obtained pattern of regulation display close similarity with the AMPK and TOR-dependent pathways, as these pathways exert antagonistic roles for storage management, autophagy, and biosynthesis whereas both activate some other pathways such as glycolysis and mitochondrial activity. However, it remains debatable whether regulation should be mediated through post-translational or transcriptional mechanisms, given that transcription-dependent or degradation-dependent changes of expression can be too slow to track environmental changes [38, 42], while rapid protein turnover can be energetically costly. Although the optimal regulatory profile of enzyme exhibited a clear and consistent pattern, the issue of optimal sensing cues remains more difficult to apprehend. An external perturbation is propagated simultaneously through both the metabolic and signaling network in a complex manner as different perturbation modes can be either amplified or attenuated in time. On the one hand, external perturbation seems to provide a more reliable cues. On the other hand, internal sensing provides informations about the metabolic state, that is how well-balanced are the respective flux [16], or how close a system is far from steady state or from the threshold beyond which metabolic collapse occurs. Combined mechanisms of ATP homeostasis and fast ATP turnover make the level of ATP:ADP:AMP ratios very sensitive to whether the metabolic stability is threatened or compromised, and such ratios therefore constitute good indicators of stress [7].

From a single-cell perspective, a primary role of intracellular signaling is to track environmental changes so as to adjust the cellular state accordingly. However, efficient metabolic adaptations in microbial organisms to environmental changes can also occur in the absence of signaling through bet-hedging strategy based on the relative growth and survival rates of cells within multistable and heterogeneous population [43]. In fact, which strategy is optimal and whether these strategies could be mixed depend on many cellular and environmental parameters, such as the rates of proliferation, the randomness and frequency of environmental changes, or the timescale and energetic cost of regulation [44–46], which is reliant on the organism’s lifestyle, prokaryote or eukaryote, unicellular or multicellular, phototroph or chemotroph. The issue of the cellular response strategy to nutrient and energy stress thus provides a promising venue for investigating the evolution of regulatory complexity.

## Acknowledgments

This work has been supported by LABEX CEMPI (ANR-11-LABX-0007) operated by the French National Research Agency (ANR).

---

---

## References

1. Lindsley JE, Rutter J. Nutrient sensing and metabolic decisions. *EMBO J.* 2004; 139: 543–559.
  2. Robaglia C, Thomas M, Meyer C. Sensing nutrient and energy status by SnRK1 and TOR kinases. *Curr Opin Plant Biol.* 2012; 15: 301–307.
  3. Yuan HX, Xiong Y, Guan KL. Nutrient sensing, metabolism, and cell growth control. *Mol Cell* 2013; 49: 379–87.
  4. Sugden C, Crawford RM, Halford NG, Hardie DG. Regulation of spinach SNF1-related (SnRK1) kinases by protein kinases and phosphatases is associated with phosphorylation of the T loop and is regulated by 5-AMP. *Plant J.* 1999; 19: 433–439.
  5. Oakhill JS, Steel R, Chen ZP, Scott JW, Ling N, Tam S, et al. AMPK is a direct adenylate charge-regulated protein kinase. *Science* 2011; 332: 1433–1435.
  6. Hardie DG, Carling D, Gamblin SJ. AMP-activated protein kinase: also regulated by ADP? *Trends Biochem Sci.* 2011; 36: 470–477.
  7. Hardie DG, Ross F, Hawley S. AMPK: a nutrient and energy sensor that maintains energy homeostasis. *Nat Rev Mol Cell Biol.* 2012; 13: 251–262.
  8. Schmelzle T, Hall MN. TOR, a central controller of cell growth. *Cell* 2000; 103: 253–262.
  9. Jacinto E, Hall MN. Tor signalling in bugs, brain and brawn. *Nat Rev Mol Cell Biol.* 2003; 4: 117–126.
  10. Dibble CC, Manning BD. Signal integration by mTORC1 coordinates nutrient input with biosynthetic output. *Nat Cell Biol.* 2013; 15: 555–64.
  11. Cunningham JT, Rodgers JT, Arlow DH, Vazquez F, Mootha VK, Puigserver P, et al. mTOR controls mitochondrial oxidative function through a YY1-PGC-1 $\alpha$  transcriptional complex. *Nature* 2007; 450: 736–740.
  12. Morita M, Gravel SP, Chénard V, Sikstrom K, Alain T, Gandin V, et al. mTORC1 controls mitochondrial activity and biogenesis through 4E-BP-dependent translational regulation. *Cell Metab.* 2013; 18, 698–711.
  13. Csibi A, Fendt SM, Li C, Poulogiannis G, Choo AY, Capski DJ, et al. The mTORC1 pathway stimulates glutamine metabolism and cell proliferation by repressing SIRT4. *Cell* 2013; 153: 840–854.
  14. Jager S, Handschin C, St-Pierre J, Spiegelman BM. AMP-activated protein kinase (AMPK) action in skeletal muscle via direct phosphorylation of PGC-1 $\alpha$ . *Proc Natl Acad Sci USA* 2007; 104, 12017–12022.
  15. Canto C, Jiang LQ, Deshmukh AS, Matakci C, Coste A, Lagouge M, et al. Interdependence of AMPK and SIRT1 for metabolic adaptation to fasting and exercise in skeletal muscle. *Cell Metab.* 2010; 11: 213–219.
  16. Kotte O, Zaugg JB, Heinemann M. Bacterial adaptation through distributed sensing of metabolic fluxes. *Mol Syst Biol.* 2010; 6:355.
  17. Khonsari AS, Kollmann M. Perception and regulatory principles of microbial growth control. *PLoS One* 2013; 10: e0126244.
-

- 
18. Zaslaver A, Mayo AE, Rosenberg R, Bashkin P, Sberro H, Tsalyuk M, et al. Just-in-time transcription program in metabolic pathways. *Nat Genet.* 2004; 36: 486-491.
  19. Chubukov V, Zuleta IA, Li H. Regulatory architecture determines optimal regulation of gene expression in metabolic pathways. *Proc Natl Acad Sci USA* 2012; 109: 5127-5132.
  20. Oyarzún DA, Stan GB. Synthetic gene circuits for metabolic control: design trade-offs and constraints. *J R Soc Interface* 2012; 10: 20120671.
  21. Oyarzún DA, Chaves M, Hoff-Hoffmeyer-Zlotnik M. Multistability and oscillations in genetic control of metabolism. *J Theor Biol.* 295: 139-153.
  22. Steuer R, Junker BH. Computational Models of Metabolism: Stability and Regulation in Metabolic Networks. In: Rice, Stuart A, editors. *Advances in Chemical Physics.* John Wiley & Sons; 2009.
  23. Covert MW, Schilling CH, Palsson B. Regulation of gene expression in flux balance models of metabolism. *J Theor Biol.* 2001; 213: 73-88.
  24. Waldherr S, Oyarzún DA, Bockmayr A. Dynamic optimization of metabolic networks coupled with gene expression. *J Theor Biol.* 2015; 365:469-485.
  25. Reznik E, Mehta P, Segrè D. Flux imbalance analysis and the sensitivity of cellular growth to changes in metabolite pools. *PLoS Comput Biol.* 2013; 9: e1003195.
  26. Liebermeister W, Klipp E, Schuster S, Heinrich R A theory of optimal differential gene expression. *Biosystems* 2004; 76: 261-278.
  27. Ingalls BP, Sauro HM. Sensitivity analysis of stoichiometric networks: an extension of metabolic control analysis to non-steady state trajectories. *J Theor Biol.* 2003; 222: 23-36.
  28. Liebermeister W. Response to temporal parameter fluctuations in biochemical networks. *J Theor Biol.* 2005; 234: 423-438.
  29. Neyfakh AA, Baranova NN, Mizrokhi LJ. A system for studying evolution of life-like virtual organisms. *Biol Direct* 2006; 1:23.
  30. Troein C, Ahrén D, Krogh M, Peterson C. Is transcriptional regulation of metabolic pathways an optimal strategy for fitness? *PLoS One* 2007; 2: e855.
  31. Gottstein W, Müller S, Herzel H, Steuer R. Elucidating the adaptation and temporal coordination of metabolic pathways using in-silico evolution. *Biosystems* 2014; 117:68-76.
  32. Milo et al. *Nucl Acids Res.* 2010; 38: D750-D753.
  33. Dejean L, Beauvoit B, Guérin B, Rigoulet M. Growth of the yeast *Saccharomyces cerevisiae* on a nonfermentable substrate: control of energetic yield by the amount of mitochondria. *Biochim Biophys Acta* 2000; 1457: 45-56.
  34. Diderich J, Teusink B, Valkier J, Anjos J, Spencer-Martins I, Van Dam K, et al. Strategies to determine the extent of control exerted by glucose transport on glycolytic flux in the yeast *Saccharomyces bayanus*. *Microbiology* 1999; 145: 3447-3454.
-

- 
35. De Jong A. *Evolutionary Computation. A Unified Approach*. Kenneth A Bradford Book. The MIT Press. Cambridge, Massachusetts. London, England.
  36. Pluskal T, Hayashi T, Saitoh S, Fujisawa A and Yanagida M. Specific biomarkers for stochastic division patterns and starvation-induced quiescence under limited glucose levels in fission yeast. *FEBS J.* 2011; 278: 1299-1315
  37. Klipp E, Heinrich R, Holzhütter HG. Prediction of temporal gene expression: metabolic optimization by redistribution of enzyme activities. *Eur. J. Biochem.* 2002; 269: 1–8.
  38. Berkhout J, Teusink B, Bruggeman FJ. Gene network requirements for regulation of metabolic gene expression to a desired state. *Sci Rep.* 2013; 3: 1417.
  39. Graf A, Schlereth A, Stitt M, Smith AM. Circadian control of carbohydrate availability for growth in Arabidopsis plants at night. *Proc Natl Acad Sci USA* 2010; 107: 9458-9463.
  40. François J, Parrou JL. Reserve carbohydrates metabolism in the yeast *Saccharomyces cerevisiae*. *FEMS Microbiol Rev.* 2001; 25: 125-145.
  41. Kaur J, Debnath J . Autophagy at the crossroads of catabolism and anabolism. *Nat Rev Mol Cell Biol.* 2015; 6: 461-472.
  42. Bennett MR, Pang WL, Ostroff NA, Baumgartner BL, Nayak S, Tsimring LS, et al. Metabolic gene regulation in a dynamically changing environment. *Nature* 2008; 454: 1119–1122.
  43. Veening JW, Smits WK, Kuipers OP. Bistability, epigenetics, and bet-hedging in bacteria. *Annu Rev Microbiol.* 2008; 62: 193-210.
  44. Kussell E, Leibler S. Phenotypic diversity, population growth, and information in fluctuating environments. *Science* 2005; 309: 2075-2078.
  45. Acar M, Mettetal JT, van Oudenaarden A. Stochastic switching as a survival strategy in fluctuating environments. *Nat Genet.* 2008; 40: 471-475.
  46. Geisel N. Constitutive versus responsive gene expression strategies for growth in changing environments. *PLoS One* 2011; 6: e27033.
-